Post-cyclic degradation of volcanic ash cohesive soils related to devastating residential damage during and after the 2016 Kumamoto earthquake

Kazuya Yasuhara[1], H. Watanabe[2], K. Kobayashi[2], Y. Arai[3], and K. Satoh[4]

[1] Institute for Global Change Adaptation Science (ICAS), Ibaraki University, Bunkyo 2-1-1, Mito, Ibaraki, 310-8512, Japan.
[2] Department of Urban and Civil Engineering, Ibaraki University, Ibaraki 312-8511, Hitachi, Japan.
[3] Kanto Branch, Chuo Kaihatsu Corporation, Kawaguchi, Saitama 332-0035, Japan.
[4] Tokyo Electric Power Services Co. Ltd. (TEPSCO), Koto-ku, Tokyo 135-0062, Japan.

ABSTRACT

To clarify the mechanisms of residential damage caused by the 2016 Kumamoto earthquake, cyclic and post-cyclic undrained triaxial tests were conducted using undisturbed volcanic cohesive soils taken from residential sites in Mashiki town, Kumamoto. Special emphasis was placed on consideration of the degradation of undrained strength and stiffness of volcanic cohesive soils based on test results, which are useful for predicting earthquake-induced settlement and displacement of residential foundations during and after earthquakes. This finding supports our understanding of the decreased bearing capacity of residential foundations and the collapse of retaining walls adjacent to residences.

Keywords: cohesive soil; earthquake; residential damage; post-cyclic degradation; triaxial test

1 INTRODUCTION

A Mj6.5 earthquake in Japan shook Kumamoto prefecture on April 14, 2016. Soon thereafter, on April 16, a Mj7.3 earthquake struck Kumamoto and Oita prefectures. A recent investigation (Yoshimi et al., 2017) revealed that nonlinearity of the seismic response for deposits layered by volcanic ash cohesive soils and pumice exacerbated the devastating damage to residences of Mashiki town near Kumamoto city during the 2016 Kumamoto earthquake. Based on those findings, the authors hypothesized that the nonlinearity of seismic response for soft deposits is associated with the cyclic degradation of strength and stiffness in deposits of cohesive volcanic ash soils, which severely damaged residences. Using simplified methods proposed by Yasuhara et al. (2001) in earlier reports of degradation characteristics of cohesive soils, the authors and others attempted to predict the residential settlement and lateral deformation of cohesive volcanic ash soils causing such severe destruction in residential areas (Yasuhara et al., 2017).

2 RESIDENTIAL SITE DAMAGE FEATURES

Devastation including 64 fatalities and 8336 complete residential failures lay in the aftermath of the 2016 Kumamoto earthquake. From a geotechnical perspective, the authors inferred at least two reasons underlying severe earthquake damage.

(i) Soil embankments used as residential foundations lost strength and stiffness, leading to collapse, severe settlement, and deformation.

(ii) Predominant nonlinearity and amplification of ground motion degraded the stiffness and strength of volcanic ash cohesive soils, leading to great degrees of lateral displacement.

Reason (ii) above was inferred as the mechanism damaging embankments and residences by rocking motions of residences and retaining walls. The damage was attributable to earthquake-induced degradation and decreased strength and stiffness of foundation soils of residences and backfill soils of retaining walls (Yasuhara et al., 2017).

3 VOLCANIC ASH SOIL FEATURES EXACERBATING RESIDENTIAL DAMAGE

3.1 Subsoil conditions at the site

The site investigation was conducted by AIST after the Kumamoto earthquake in the Miyazono district in Mashiki town in Kumamoto, which

exhibited the most severe damage. It has deposits of soft volcanic ash cohesive soils covered by a loam layer and an embankment.

3.2 Index properties of volcanic ash-cohesive soils

Fig. 1 presents the soil profile for the location where AIST sampling was conducted. Before dynamic triaxial shear deformation tests and post-cyclic monotonic triaxial tests at the laboratory, index tests were conducted of volcanic ash cohesive soils sampled from the site shown in Fig. 1.

According to results from both index tests (ρ_s = 2.756–2.771 g/cm^3; w_i = 63.3% – 74.2%; I_p = 31.1–35.0), soil specimens were classified as compressible silt-rich (approximately 50%) cohesive soils (VH_1-S or MHS-G) with low strength (Yasuhara et al., 2017). Therefore, we inferred that these volcanic-ash cohesive soils are related to the severe residential damage shown in Mashiki town during the earthquakes.

The shear modulus and shear strain relations were obtained from dynamic triaxial deformation tests (Yoshimi et al., 2017). The authors suspect that the nonlinearity of ground response at and subsequent ground motion amplification softened the volcanic ash cohesive soils, causing severe damage to residences (Yasuhara et al., 2017) during the earthquakes, and that ground motion amplification softened the volcanic ash cohesive soils, causing severe damage to residences (Yasuhara et al., 2018).

were investigated using procedures proposed by Yasuhara et al. (2001) in earlier reports. They include undrained cyclic triaxial tests followed by undrained monotonic tests, as presented in Fig. 2.

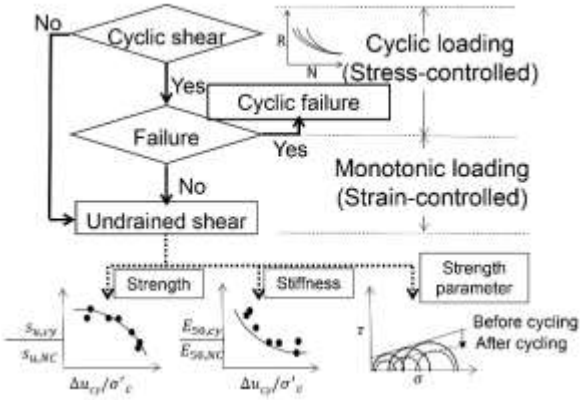

Fig. 2. Testing procedures for cyclic and post-cyclic tests.

Fig. 3 schematically portrays stress vs. strain curves with and without undrained cyclic loading. The undrained strength was ascertained from half of the maximum principal stress difference, as $(\sigma_1-\sigma_3)_{max}/2$, although the secant modulus was found from the gradient of the straight line passing through this coordinate and the point corresponding to half of the maximum principal stress difference, designated as $(\sigma_1-\sigma_3)_{max}/2$.

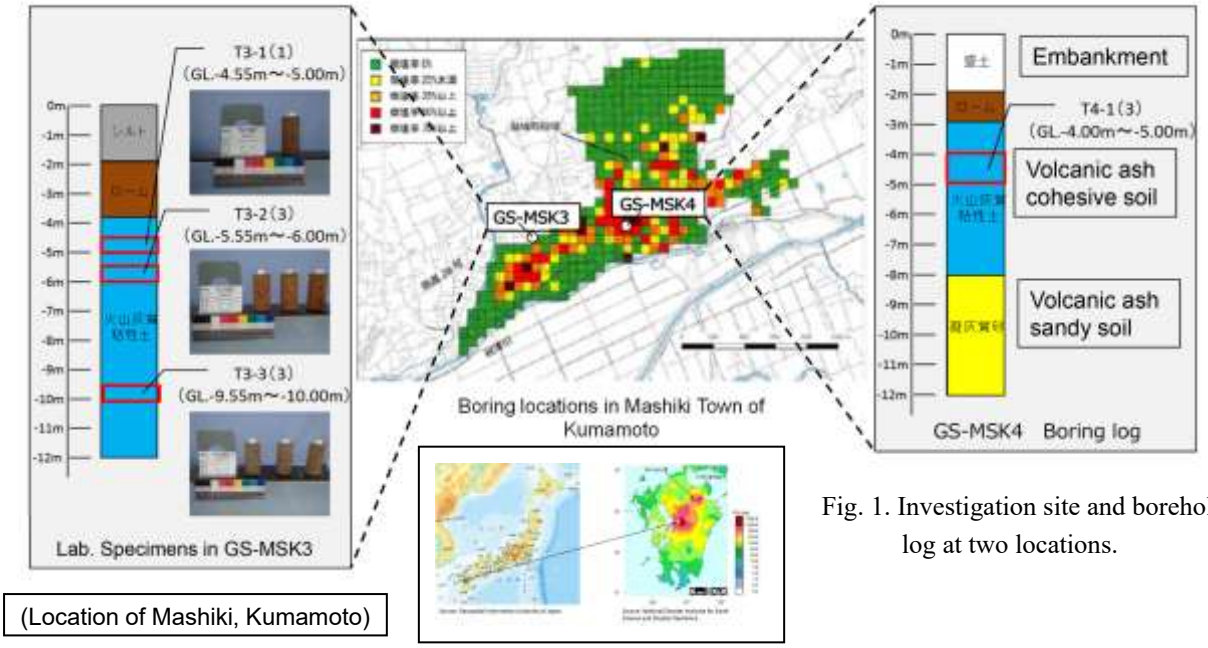

Fig. 1. Investigation site and borehole log at two locations.

4 POST-CYCLIC TRIAXIAL TESTS

4. 1 Testing procedures

Post-cyclic degradation of strength and stiffness

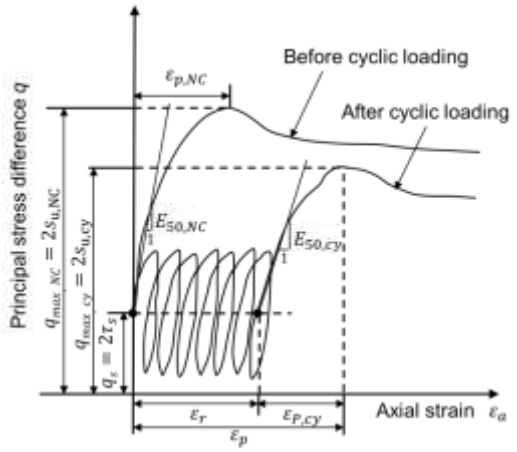

Fig. 3. Key sketch for stress vs. strain in cyclic and post-cyclic tests.

The test scheme is characterized as described below.
i) Cyclic stress ratio τ_{cy}/σ'_c of 0.25–0.35 and the number of load cycles from 1 to 58 were combined as testing conditions.
ii) The testing program is planned to combine the normalized cyclic shear stress τ_{cy}/σ'_c and the number of cycles under the constant cyclic frequency f equal to 10 s /cycle to obtain widely various normalized excess pore pressure $\Delta u_{cy}/\sigma'_c$ of 0 through 1.0, which is generated during undrained cyclic loading.
iii) The double amplitude axial strain ε_{DA} generated during undrained cycling is not large (3.5% at most), but the maximum value of the normalized excess pore pressure becomes nearly 0.9.

4.2 Change of strength parameters caused by undrained cyclic loading

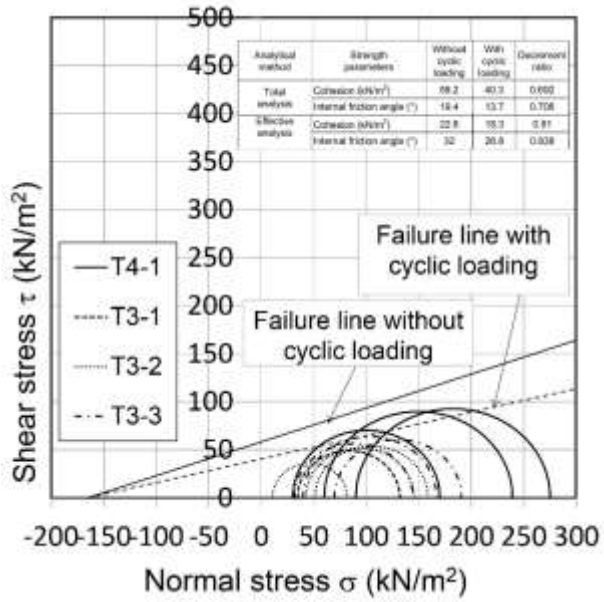

Fig. 4. Mohr circles for total stress analysis.

A set of Mohr circles in terms of both total and effective stress analysis obtained from results of post-cyclic undrained triaxial tests is depicted for comparison with results from monotonic triaxial tests on undisturbed specimens with no cyclic loading experience under confining pressures of 65, 75, and 90 kPa. The results portrayed in Fig. 4 indicate a decrease in strength parameters c and ϕ in total stress analyses. A noteworthy characteristic is that the decrement in cohesion is more readily apparent than the decrement in the internal friction angle.

4.3 Change of undrained strength and undrained stiffness

Stress–strain relations in post-cyclic monotonic loading are portrayed in Fig. 5. Following the procedure explained earlier, the undrained strength s_u and undrained secant modulus E_{50} were ascertained from those stress–strain curves.

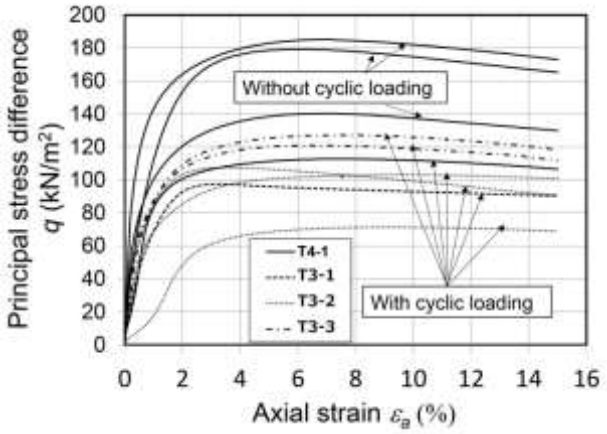

Fig. 5. Post-cyclic stress–strain relations.

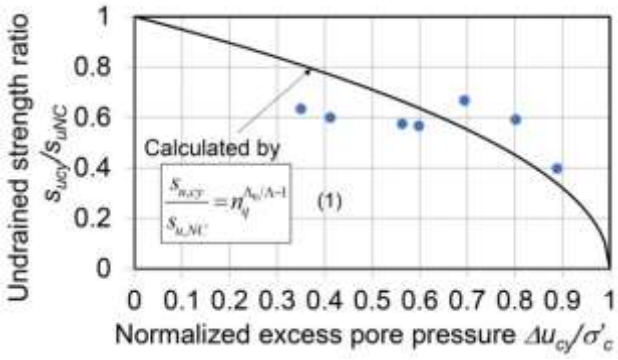

Fig. 6. Post-cyclic degradation of undrained strength.

The results are shown against the normalized excess pore pressure generated during undrained cyclic loading in Figs. 6 and 7, where black circles and squares represent data obtained from stress–strain curves in Fig. 5. Thick lines present results calculated using theoretical relations given as

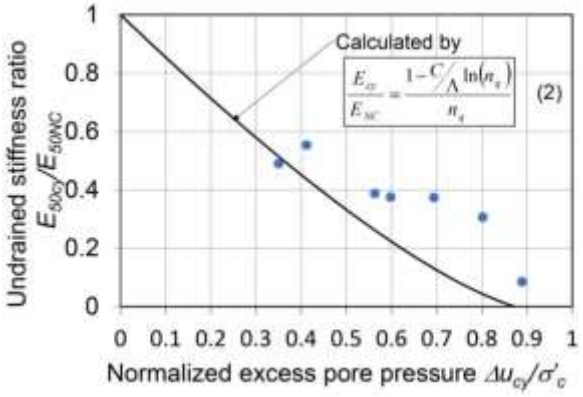

Fig. 7. Post-cyclic degradation of undrained stiffness.

$$\frac{s_{u,cy}}{s_{u,NC}} = n_q^{\Lambda_0/\Lambda-1} \quad (1), \qquad \frac{E_{cy}}{E_{NC}} = \frac{1-C/\Lambda \ln(n_q)}{n_q} \quad (2)$$

Parameters included in Eqs. (1) and (2) are defined as shown below.

$$n_q = 1/(1-\Delta u_{cy}/\sigma'_c) \quad (3)$$

$$\Lambda_0 = \frac{\log\{(s_u/p')_{OC}/(s_u/p')_{NC}\}}{\log OCR} \quad (4)$$

$$\Lambda = 1 - C_s/C_c \quad (5)$$

Furthermore, the parameter in Eq. (2) is given as described by Wroth and Houlsby (1985).

$$C = \frac{(E/p')_{OC}/(E/p')_{NC}-1}{\ln OCR} \quad (6)$$

No data for oedometer tests or for undrained tests on overconsolidated specimens are available. Therefore, the parameters stated above were determined as parameters of the plasticity index as presented in Table 1 (Yasuhara et al. 2001; 2017).

Table 1. Experimental parameters used for calculation.

Parameter	Symbol	Unit	Figure
Irreversible parameter	Λ	-	0.635
Strength change parameter	Λ_0	-	0.745
Stiffness change parameter	C	-	0.26
Compression index	C_c	-	0.602
Recompression index or swelling index	C_r or C_s	-	0.135
Undrained strength	s_u	kN/m^2	89.75
Secant modulus	E_{50}	MN/m^2	27.16

Roughly speaking, overall agreement is apparent between the calculated and observed results for the decreasing tendency of post-cyclic undrained strength and stiffness with increasing excess pore water pressure generated during undrained cyclic loading. Results also demonstrate that the decrease in post-cyclic undrained secant modulus is greater than that of the post-cyclic undrained strength.

5 CONCLUSION

Cyclic and post-cyclic undrained triaxial tests were conducted on undisturbed volcanic cohesive soils from residential sites in Mashiki town, Kumamoto. Special emphasis was placed on the consideration of degradation of undrained strength and stiffness of volcanic cohesive soils based on the test results, which are useful for predicting earthquake-induced settlement and displacement of foundations of residences during and after earthquakes. Results of post-cyclic undrained strength and stiffness of observed in triaxial tests agree well with those predicted using the methodology the authors proposed earlier.

ACKNOWLEDGEMENTS

Research for this study was supported financially by a Grant-in-Aid (No.16H02362) from MEXT to the first author. The samples used were kindly provided by Dr. Yoshimi, Senior Researcher of AIST, Japan. The authors express their sincere gratitude for these support and cooperation.

REFERENCES

Wroth, C. P. and Houlsby, G. T. (1985). Soil mechanics – Property characterisation and analysis procedures. Proc. 11th ICSMFE, 1, 1-56.

Yasuhara, K., Murakami, S. Toyota, N., and Hyde, A. F. L. (2001). Settlements in fine-grained soils under cyclic loading. Soils and Foundations, J. of JGS, 41(6), 25-36.

Yasuhara, K., Watanabe, H., Kobayashi, K., Yoshimi, M., Arai, Y., Hosoya, S., M. Tajiri, S., and Murakami, S. (2017). Instability of residences founded on volcanic cohesive soils during the 2016 Kumamoto Earthquake, Lowland Technology International, 19(3), 205-216, International Association of Lowland Technology (IALT): ISSN 1344-9656

Yoshimi, M., Goto, H., Hata, Y., and Yoshida, N. (2017). Nonlinear site response at the worst-hit area of the 2016 Kumamoto earthquakes in the Mashiki town, Kumamoto, Japan, DPRI Kyoto University Annual Meeting 2017, A05 (in Japanese).